Proceedings World Geothermal Congress 2020+1
Reykjavik, Iceland, April - October 2021

3D Numerical Modelling Combined with a Stochastic Approach in a MATLAB-based Tool to Assess Deep Geothermal Potential in Catalonia: The Case Test Study of the Reus-Valls Basin

Ignasi Herms[a], Guillem Piris[b], Montse Colomer[a], Charlotte Peigney[a], Albert Griera[b], Juanjo Ledo[c]

[a] Institut Cartogràfic i Geològic de Catalunya (ICGC), Parc Montjuïc E-08038, Barcelona, Spain

[b]Departament de Geologia. Universitat Autònoma de Barcelona (UAB) 08193 Cerdanyola del Vallès, Barcelona, Spain

[c] Facultat de Ciències de la Terra, Universitat de Barcelona (UB), Martí i Franqués, s/n, 08028 Barcelona, Spain

ignasi.herms@icgc.cat, guillem.piris@uab.cat, montse.colomer@icgc.cat

Keywords: Volumetric method, resource assessment, 3D modelling, stochastic approach, MATLAB

ABSTRACT

This paper presents the test phase results of a new MATLAB script to evaluate deep geothermal resources from 3D voxel-based geologic models which consider the USGS volumetric 'heat in place' method combined with Monte Carlo simulations. The case test study is located in the Reus-Valls basin (Catalan Coastal Range, NE Iberian, Spain), a rift basin formed during the Cenozoic opening of the Western-Mediterranean. According to previous studies, the selected area has a high potential to develop deep geothermal projects. In this sense, the area has been selected to test the workflow presented in this paper which has the aim to easy assessing deep geothermal resources in a friendly way by combining 3D modelling techniques and stochastic approaches. Firstly, a 3D implicit geological model combined with a full gravity/magnetic litho-constrained stochastic geophysical inversion analysis was built using 3DGeoModeller software (©BRGM, Intrepid-Geophysics). Secondly, a steady-state, 3D conductive heat flow model applying a heat uncertainty analysis of the basin was developed to estimate the probable temperatures in place at one of the main hot sedimentary aquifers. Finally, through a new MATLAB script that works firstly by the outputs from 3D voxel-based models and by applying the heat in place method combined with Monte Carlo simulations, has allowed to quantify the geothermal resource base and produce different maps of the in terms of P10, P50 and P90 of probability (in MWt).

1. INTRODUCTION

Since the last decade, deep geothermal energy exploration and exploitation is increasing enormously worldwide. To develop projects, one of the key points in the first phases is the quantification of deep geothermal base resources in terms of energy stored in the reservoir. But to perform a preliminary assessment of geothermal resources available at the early stages of exploration, there is always an uncertainty in the geological knowledge that must be considered.

In deep geothermal potential assessment, the USGS volumetric "Heat In Place" (HIP) method (Muffler and Cataldi, 1977) is commonly used to evaluate the stored heat. This method combines the reservoir volume with the petrophysical rock properties (considering both the rock body and the fluids that could be contained in it) as well as the reservoir temperature and the reference or reinjection temperature to assess the stored heat. This method by itself is sensitive with some parameters normally little-known at early stages of exploration, as the reservoir geometry, the petrophysical rock values or the percentage relationship between the rock body and contained fluids (porosity). Due to the existing uncertainty with these parameters, the HIP method is normally combined with a stochastic approach like the Monte Carlo simulation by allowing the parameters to vary over a defined range by using probability distribution functions (PDF) (triangular, normal, lognormal, etc.) (e.g. Garg and Combs, 2015).

The approach followed in this work combine the construction of 3D voxel-based geological and thermal models and the application of the HIP method combined with Monte Carlo simulations that work from their outputs. The application of the HIP method was implemented through a new MATLAB-based tool which is firstly tested in this work. This tool allows getting the HIP results considering all the volume of the reservoirs modelled in 3D as well as producing maps in GIS format where the HIP distribution across the reservoir can be visualised. The results are expressed in probability terms of P10 (very low confidence of the estimation and high values), P50 and P90 (high confidence of the estimation and low values).

To test the mentioned workflow, we used the Reus-Valls Basin (RVB), which is part of a set of SW-NE oriented extensional basins in the Catalan Coastal Ranges (NE of the Iberian Peninsula). This basin, according to previous works (ICGC, 2012; Colmenar-Santos et al., 2016) has a high potential for the development of deep geothermal energy for direct heat or power production, both in different hot sedimentary deep aquifers and in fractured crystalline rocks. However, the lack of enough subsurface data (geophysics and deep wells), produced a large uncertainty in the assessment of geothermal potential in the basin. The analysis in this paper has focused on the Lower Triassic conglomerates and sandstones (Buntsandstein). The first aim of this work was to build a first 3D geological model (3DGM) using a full gravity/magnetic litho-constrained stochastic geophysical inversion approach. Then, the 3DGM was used to construct a steady-state 3D conductive heat flow model applying a heat uncertainty analysis. This allowed estimating the probable temperature distribution, obtaining a 3D temperature model (3DTM). Finally, both 3DGM and 3DTM were combined to calculate the HIP through the volumetric method using the new MATLAB script.

2. METHODOLOGY

In this section, the workflow followed to construct 3D models and evaluate the "Heat in Place" is shown. Although this work presents a preliminary result, it has to be taken into account that the geological model is still improving with the incorporation of new field

data, so the results must be considered as preliminary. The workflow will be reused at a more advanced stage of 3D modelling for the final evaluation of deep geothermal potential in this area and other ones.

2.1 Workflow for 3D Geological and Geophysical Modelling

The first aim of this work is to generate a preliminary 3D geological model (3DGM) from currently available data. In this case, it is used the potential-field interpolation and geological rules within the implicit approach of 3DGeoModeller software.

In order to build up the 3DGM several data can be used: surface data (dip/azimuth measurements), geological maps, previous 3D modelled surfaces, data from shallow and deep wells, geophysical data 8seismic profiles, etc.). Thus, all these data must be integrated obtaining a first preliminary 3D Geological Model. The model will be then validated according to available geophysical potential-field data (gravity and magnetics) by means of forward modelling and geophysical inversion by full gravity / magnetic litho-constrained stochastic approach. So, at this stage, petrophysical properties (rock density and magnetic susceptibility) have to be considered for each rock formation. The 3D inversion modelling approach is applied to fit the most probable 3D geological model through a stochastic approach. The result is a 3D Probabilistic Geological Model (Figure 1), which should honour all the data, and from which can be derived a 3D voxel model which could be used afterwards to follow 3D thermal modelling analysis.

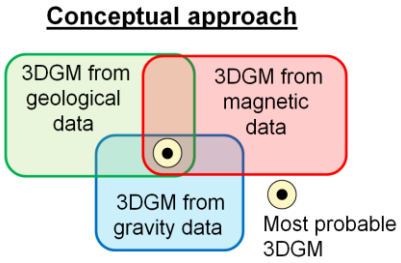

Figure 1: Conceptual approach for 3D geological and geophysical modelling.

2.2 Workflow for 3D Thermal Modelling

Once we have performed the 3DGM, the next step is to build a 3DTM (thermal model). In the case of conduction dominated the heat transport, it can be used the 3DGeoModeller software using the "*Forward Model Temperature*" module. If convection dominates the heat transport n the domain, other software like TOUGH2 or FEFLOW should be used. The workflow presented is based on 3DGeoModeller, and the Parameter Sweep - Heat resource uncertainty algorithm. This algorithm solves the heat transport equations in steady-state considering conduction, and it calculates the isotherms for the entire domain following a quasi-stochastic approach: It uses Dirichlet (fixed-temperature) or Neumann (fixed heat flow) boundary condition at the top and at the bottom, and considering for each lithology, the variation of the parameters - thermal conductivity (W/m·K) and heat production rate (W/m^3) – specifying the mean value and the corresponding standard deviation. Thus, all the elements of the simulation with no zero standard deviation can be perturbed along with the simulation generating different 3DTM's. However, unlike a typical stochastic evaluation where n random values are taken from a distribution, 3DGeoModeller only uses three different values for each variable: mean + standard deviation (Sd), mean, mean – Sd. Considering that, with two variables and their Sd, you will obtain 3^2 different 3DTM's (3 = permutations number and 2=n=variable number). Finally, 3DGeoModeller compile in a unique model all these 3DTM solutions. The way to compile the different 3DTM is calculating the mean and Sd for the solutions distribution, i.e., for the 3^n models.

The result of step 2.1 and 2.2. are exported as 3D voxel-based models which will contain: the reservoir inferred temperature, the lithology (based on the 3DGM results), the voxel position (X, Y, Z coordinates) and the rock densities (derived from the geophysical inversion process).

2.3 Workflow for the Geothermal Resource Assessment Using 3D Models and Monte Carlo Simulations

To assess the deep geothermal potential for any target, the volumetric Heat in Place (HIP) method (Muffler and Cataldi, 1977) will be applied at each voxel from the resulted 3D voxel-based model.

$$HIP = V \cdot [\emptyset \rho_W C_W + (1 - \emptyset)\rho_R C_R] \cdot (T_R - T_r) \quad \textbf{(1)}$$

where V is the reservoir volume (voxel size m^3), $\emptyset$ is the porosity (dimensionless), ρ is the density (Kg/m^3), and C is the specific heat (KJ/kg·ºC) - the sub-index W or R indicate water or the rock grains respectively. The T_R is the average reservoir temperature (ºC), and T_r is the reinjection or reference temperature (ºC).

The HIP method combined with probabilistic Monte Carlo simulations allows considering the reservoir uncertainties or heterogeneities as for example the porosity, rock density or the specific heat (Garg and Combs, 2010; Garg and Combs, 2011). Thus, each parameter can be defined by a probability distribution (normal, triangular, lognormal, etc.) and the stored heat can be evaluated by a probabilistic way obtaining a probability curve of the stored heat, from which the P10 (very low confidence of the estimation and high values), P50 and P90 (high confidence of the estimation and low values) can be extracted.

2.3.1 The MATLAB script

In order to apply the HIP method using Monte Carlo simulations, it has been coded a new MATLAB script able to perform the simulations, compile the results and getting different graphs and maps with the results.

The following scheme shows in an easy way how the code runs (Figure 2). First, the code extracts the density and the temperature and temperature Sd from the 3DGM and the 3DTM respectively and ask the user how many simulations wants to compute. Then, the code gives the user the possibility to select the lithology that will be evaluated from the different layers defined on the 3DGM. After the lithology is selected, it shows a plot with the depth temperature distribution of this layer (data derived from the 3DTM), giving the user the possibility to select a specific depth range for the analysis (e.g. the Triassic lithology between -2200m and -2400m). The next step is to introduce the HIP parameters for the selected lithology (porosity, fluid density, specific heat for the rock and fluid within the pores) with a mean value and the related Sd. Using all the introduced parameters, the code automatically computes as many HIP simulations as the user-defined, using as input parameters random values from the normal distributions generated by the mean and Sd values of each parameter (In the current beta test version, the code uses normal distributions. For future versions, the user will be able to select which distribution want to use normal, triangular or lognormal). The result of this step is a matrix with as many rows as selected cells (e.g. all the cells of Triassic lithology between -2200m and -2400m) and as many columns as HIP simulations number were selected. The sum of all rows is the HIP distribution for the entire reservoir, and its compilation is the cumulative probability curve and from it the P10, P50 and P90 values.

Furthermore, the code also shows some histograms of the selected cells as for example, the temperature, depths and densities. Finally, and to see the results in a map format, it computes the P10, P50 and P90 for each cell and sums all the Z values with the same X and Y plotting the results in PJ/Km^2 (e.g. P10 HIP in PJ/Km^2 of Triassic between -2200m and -2400m). Additionally, the code also exports files with the obtained results to be plotted with Geographic Information System (GIS) software.

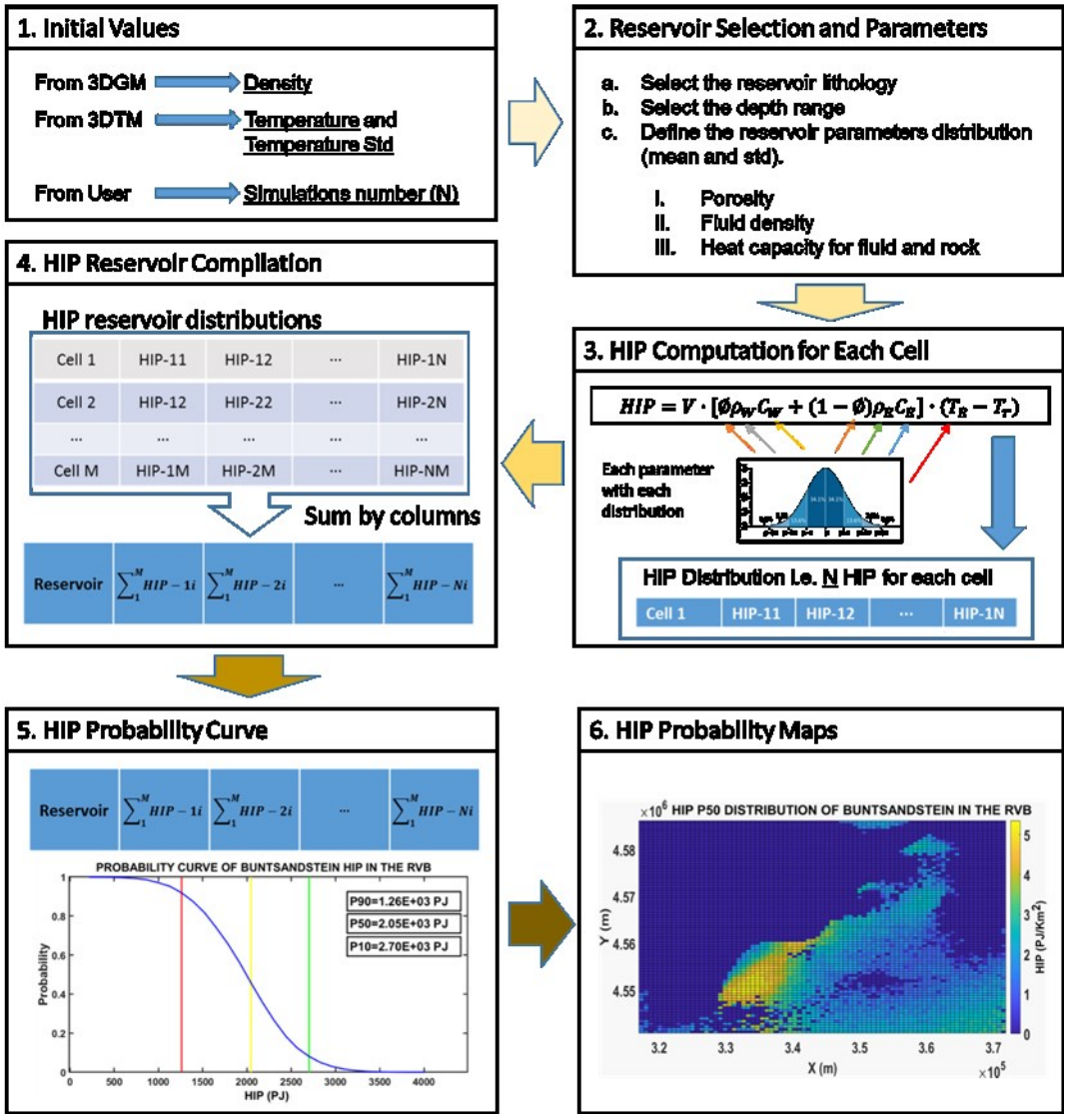

Figure 2: Flow diagram with the steps run by the script (MATLAB script, beta version July 2019)

3. THE CASE STUDY OF THE REUS-VALLS BASIN

3.1 The Geological and Geothermal Setting

The Reus-Valls Basin (RVB) is part of a set of SW-NE oriented extensional basins in the Catalan Coastal Ranges (Figure 3A), which originated during the Neogene rifting episode related to the opening of the Valencia Trough. The basin shows a half-graben geometry strongly tilted towards its NW margin, where it is limited by the Camp Fault, which controls the basin depocenters (Masana, 1995). The Camp Fault is an extensional NE-trending, SE-dipping basement fault (Cabrera and Calvet, 1996) that was active from the early

Miocene to the Quaternary. The fault separates the Prades-Llaberia and Miramar ranges (where the Mesozoic cover and the Palaeozoic basement rocks outcrop) from the basin's Neogene sedimentary infill, which reaches an estimated maximum thickness of about 2000 m near la Selva del Camp and Montbrió (Masana, 1995).

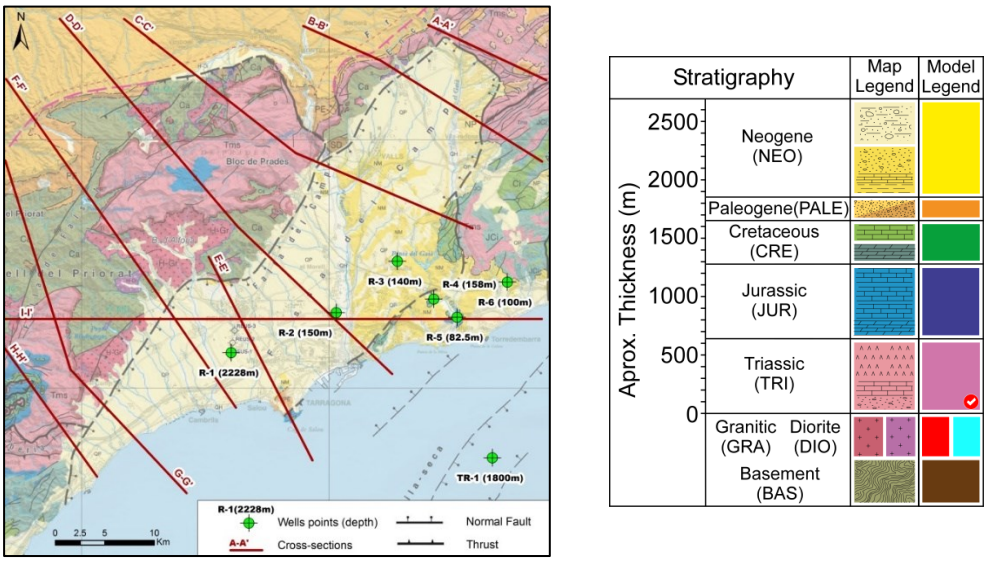

Figure 3: A) (left) Structural map of the study basin (ICGC, 2014). Map also shows the cross-sections and the locations of the borehole data used to build the 3DGM; B) (right) Stratigraphic pile for the ICGC (2014) map, and the 3DGM. Red 'click' indicates the tested geothermal target of this work (the fractured sandstones of the Buntsandstein).

Inside the basin, the Neogene sediments entirely bury the Mesozoic and the Palaeozoic basement unconformably. Paleogene deposits are not present inside the RVB; this unit lies unconformably on top of the Mesozoic series in the Ebro Basin, in the NW area of the model. The regional lithostratigraphic succession (Figure 3B) in the area, from deepener to shallower rocks, is the following (IGME, 1973; IGME, 1980):

- Palaeozoic metasedimentary series of Silurian to Carboniferous rocks, partially affected by contact metamorphism caused by tardi-Variscan plutonic intrusions (tonalites, diorites, granodiorites).
- Lower Triassic rocks composed by Buntsandstein facies: red detrital series formed by heterometric conglomerates and fine sandstones, grading to mudstones to the top.
- Middle Triassic Muschelkalk facies, defined by two carbonated intervals of limestones and dolomitised limestones with an intermediate level of continental red fine sandstones, mudstones and gypsum layers.
- Upper Triassic, defined by Keuper facies: Versicolor claystone with interlayered gypsum levels are observed in the southern part of the basin, while finely stratified dolomites and yellow claystone are present to the northern part of the basin.
- Jurassic carbonates that can be subdivided into (a) a lower and intermediate calcareous unit formed by Liassic brecciated dolostones and Dogger marly limestones and dolostones; and (b), an upper unit of Malm intensely karstified dolostones.
- Cretaceous carbonated series, mostly made of limestones, with intercalations of dolomites and marly limestones.
- Paleogene unit of detrital sediments, mainly sandstones and conglomerates.
- Finally, the Neogene sedimentary cover, with a detrital basal unit of carbonated breccias and conglomerates unconformably overlying the Mesozoic succession. The next unit is made of marine and transitional units of boundstones (i.e. reef environment facies), marls and carbonated conglomerates alternating with sandstones, becoming continental again at the top with mudstones, sandstones and conglomerates (Masana, 1995).

As mentioned, RVB is the product of the Oligocene, and Neogene extensional continental margin occurred in the Valencia trough. In consequence, it shows the same structure as the Catalan margin where the basin is located: a typical continental margin structure with a relatively thin crust (Ayala et al., 2015a) with a well-developed horst and graben structure. In the other hand, there is no recognised any magmatic or hydrothermal circulation inside the tested zone. So, it should expect that heat transport into the basin is dominantly controlled by the thermal conductivity of the reservoir rock, which relates to the lithofacies and/or biofacies subdivisions within the basin fill sequence. This is a conduction dominated play type in an intracratonic basin and responds to a CD-1 in the catalogue of Moeck-Beardsmore Play Types (Moeck, 2014). In this case, the reservoir rocks to be considered, which are confined in the deepest parts of the basin, are the fractured sandstones and conglomerates of The Buntsandstein (indicated with a red icon in Figure 3B). This presents a thickness between 60-130 m in the outcrops in this area (Marzo, M., 1980).

3.2 The 3D Geological and Geophysical Model

To construct the 3DGM for the RVB, we did the following steps. Firstly, a preliminary 3DGM was generated using all the available data such as the Digital Terrain Model (MDT), surface geology information (dip/azimuth data), regional geological maps (ICGC, 2014), data from the surface-based 3D geological model of Catalunya (ICGC, 2013), old cross-sections, Reus-1 deep oil/gas borehole (BTH depth -2228m and Z: 74.26 m a.s.l.), interpreted horizons from 2D old seismic profiles. Figure 4 summarises the distribution of the surface and subsurface geological data used to build the 3D geological model.

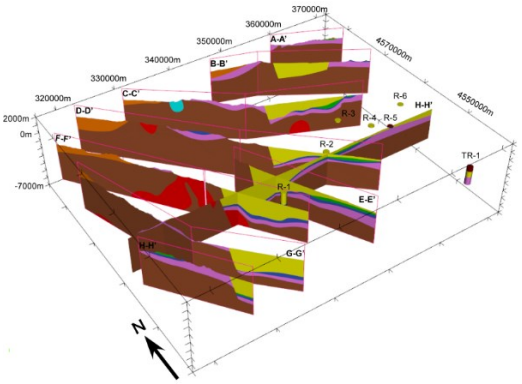

Figure 4: Initial cross-sections from geological and well data. Location of cross-sections and lithological legend is equivalent to that shown in Figure 3 A and B.

However, to refine this preliminary 3DGM, a full gravity/magnetic litho-constrained stochastic geophysical inversion approach using the 3DGeoModeller software is used. At this stage of the project, bibliography petrophysical properties are used (Table 1): the density values were extracted from a gravity inversion model performed near the study area (Ayala et al., 2015b) and the magnetic values were extracted from general bibliography (Clark, 1997). However, to well fix the petrophysical values for new sampling campaigns are ongoing actually in the study area.

Lithology	Rock density (g/cm^3)		Magnetic susceptibility ($SI \cdot 10^{-6}$)	
	M	**Sd**	**M**	**Sd**
NEO	2.4	0.2	200	20
PALE	2.5	0.2	100	10
CRE	2.56	0.3	100	10
JUR	2.62	0.1	200	20
TRI	2.5	0.2	34	4
GRA	2.67	0.15	3420	342
DIO	2.67	0.15	12500	550
BAS	2.68	0.15	280	28

Table 1: Loaded rock properties. (M – Mean value / Sd. Standard deviation) (Ayala et al., 2015; Clark, 1997).

To perform the gravity / magnetic inversion 5e6 iterations were applied, obtaining an acceptable misfit for the gravity and magnetic fields (Figure 5). The post-inversion misfit for the gravity was very low, just the region near the Camp Fault was showing a no perfect adjustment. However, the magnetic results showed higher values through all the area, with peak values near the plutonic outcrops, the fact that potentiates the necessity to perform field works to better capture the petrophysical parameters, with special attention on the magnetic values. Together with the post-inversion misfits, the 3DGeoModeller software gives, as a result, the post-inversion 3DGM in a 3Dvoxet format where each cell has the lithology information and petrophysical values (Figure 6). These petrophysical values normally are slightly been modified during the inversion process to improve the lithology response; these modifications are concentrated around the lithology contacts were the geological uncertainty is higher. Additionally, 3DGeoModeller outcomes the final 3Dvoxel entropy model which gives information about the geological model uncertainty (Wellmann and Regenauer-Lieb, 2012). The results showed that high entropy regions are associated with the top of the basement and the granitic bodies (Figure 6 B).

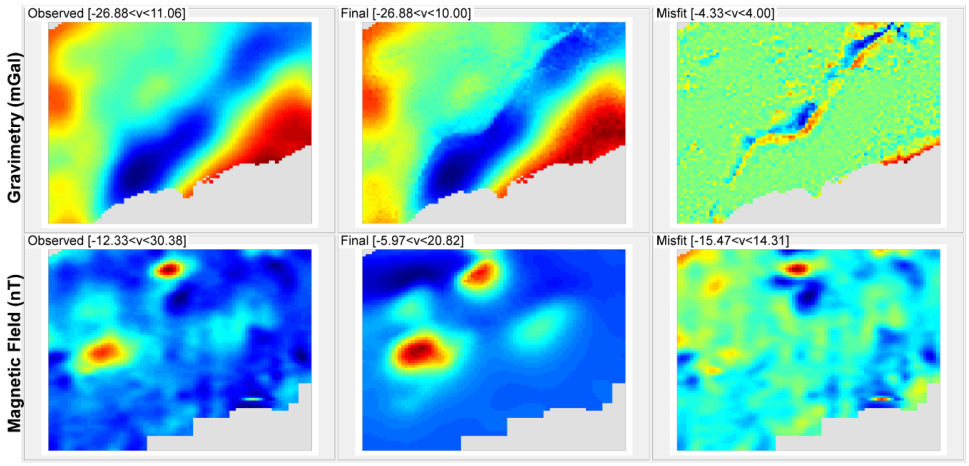

Figure 5: Final post-inversion Misfit for gravity and magnetic data. In the first column, there are the observed gravity and magnetic anomaly; in the second column, the 3D geology gravity and magnetic anomaly response; and in the third column, their equivalent Misfits.

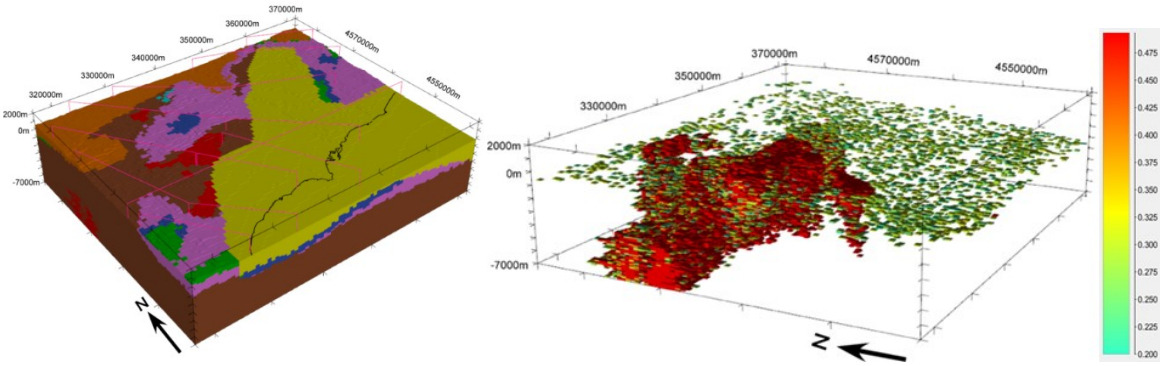

Figure 6: A) Final post-inversion discretised 3DGM. The black line represents de shoreline, and the colour legend is equivalent to that shown in Figure 3. B) 3D voxel entropy model and the final granitic bodies (red) within the final 3DGM.

3.3 The 3D Thermal Model

Once the 3DGM was already built, we used the 3Dvoxel-based geological model result of the gravity / magnetic inversion to perform a 3DTM using the conductive equations and the 3DGeoModeller temperature module. The thermal parameters for each lithology (Table 2) and thermal boundary conditions - surface temperature of 15ºC and base temperature at 7Km depth of 176ºC - were used as inputs for the conductive calculations. Depth temperature value was extracted from the regional temperature gradient of 23ºC/Km (Fernàndez, M, 1988), and thermal properties, as well as the heat production rate, were extracted from the bibliography (Čermák and Rybach, 1982; Hasterok et al., 2018). As the Table 2 shows, only the basement thermal conductivity and the granite heat production rate have Sd different of 0, so we obtained nine 3DTMs that were compiled statistically to obtain the final 3DTM (Figure 7). The final 3DTM was a 3D voxel model containing for each cell all the thermal properties and the associated Sd, as well as the cell temperature and the associated Sd.

Lithology	Thermal conductivity (W/m·K)		Heat production rate (W/m^3)	
	M	**Sd**	**M**	**Sd**
NEO	2.6	0	5e-7	0
PALE	2.6	0	5e-7	0
CRE	2.3	0	5e-7	0
JUR	2.3	0	5e-7	0
TRI	2.7	0	5e-7	0
GRA	3.0	0	2.7e-6	1e-6
DIO	3.0	0	2.7e-6	0
BAS	3.5	0.2	5e-7	0

Table 2: Thermal and heat production properties (M – Mean value / Sd. Standard deviation) (Cermak and Rybach, 1982; Hasterok et al., 2018).

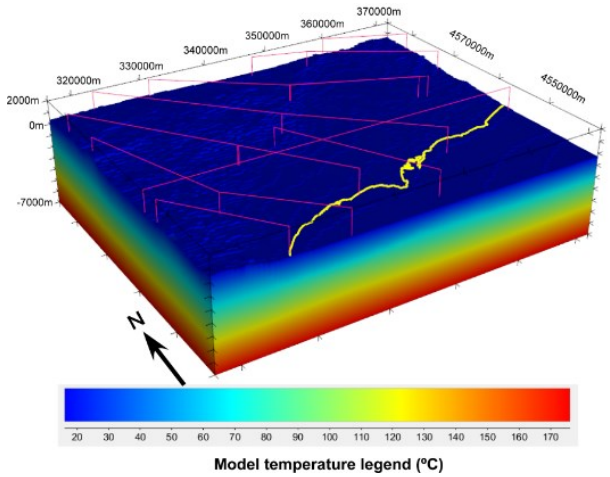

Figure 7: Final 3D thermal model for the Reus-Valls basin case. The yellow line represents the shoreline.

3.4 Assessment for Geothermal Energy Within Deep Aquifers in the Reus-Valls Basin:

Once the 3DGM and the 3DTM were constructed for the Reus-Valls basin, the next step was evaluating the HIP with Monte Carlo simulations for the units that could be considered as possible geothermal targets. In this case, we focused on the Buntsandstein unit inside the Triassic series. This unit is stratigraphically located at the bottom of the Triassic series and for the study area is conformed by sands and conglomerates with a thickness between 60 and 130 m (Marzo, 1980). Besides, to apply the HIP method, we considerate an estimate mean porosity of 0.11 to 0.15 filled by brine (with a salinity of 32gr/l, Aurensa, 1996). The physical properties of the Buntsandstein sands and conglomerates layer are shown in Table 3. The density value for the HIP calculation was provided by the 3DGM where was defined for each cell. Finally, to run the MATLAB script we defined 10000 simulations for the HIP Monte Carlo

evaluation, and we only considered the Buntsandstein located between the -4000m and -1000m depth, and we defined 30ºC as the reinjection temperature (T_r).

Petro-physical parameters considered for the Buntsandstein			
Parameter	**Mean**	**Sd**	**Reference**
Brine density (kg/m^3)	1025	15	Oldenburg and Rinaldy (2010)
Brine specific heat (KJ/kg·ºC)	3.9	0.1	Lukosevicius (1993)
Porosity	0.12	0.03	Gomez-Gras (1992)
Rock specific heat (KJ/kg·ºC)	0.75	0.05	Willems and Nick (2019)

Table 3: Physical properties for the Buntsandstein unit.

3.4.1 Results

The HIP results were plotted in a cumulative probability HIP distribution where P10, P50 and P90 could be extracted (Figure 8A). Additionally, the MATLAB-based tool also allows seeing some distributions about the selected layer such as density, mean temperature (Figure 8 B) or depth. However, these results considered the whole Buntsandstein of the basin between -1000 and -4000m (range considered to capture all the whole Buntsandstein from the 3DGM), and maybe it is difficult to identify in which regions this layer have a higher potential. For that, the results were also plotted in distributed map format where the HIP was expressed in terms of energy per area unit (PJ/Km^2) with a probability of P10, P50 (Figure 9) and P90.

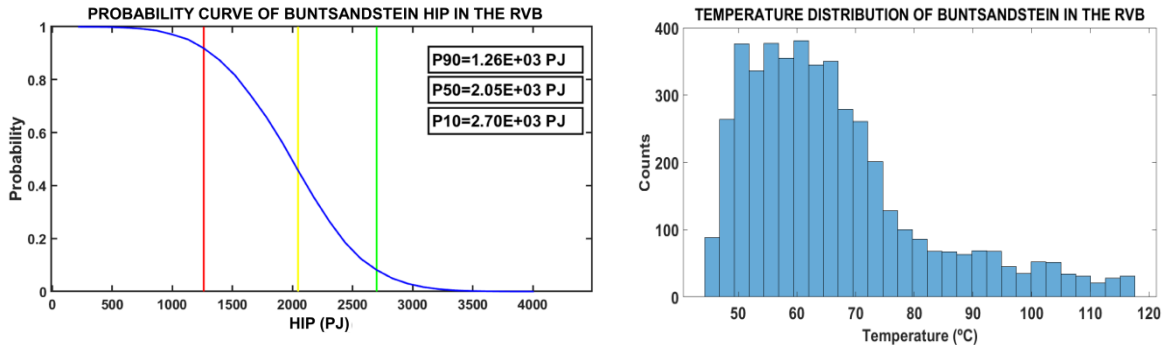

Figure 8: A) (left) Probability curve of Buntsandstein HIP between -1000 and -4000m depth in the Reus-Valls Basin (RVB). B) (right). Temperature distribution of the Buntsandstein in the RVB between -1000 and -4000m.

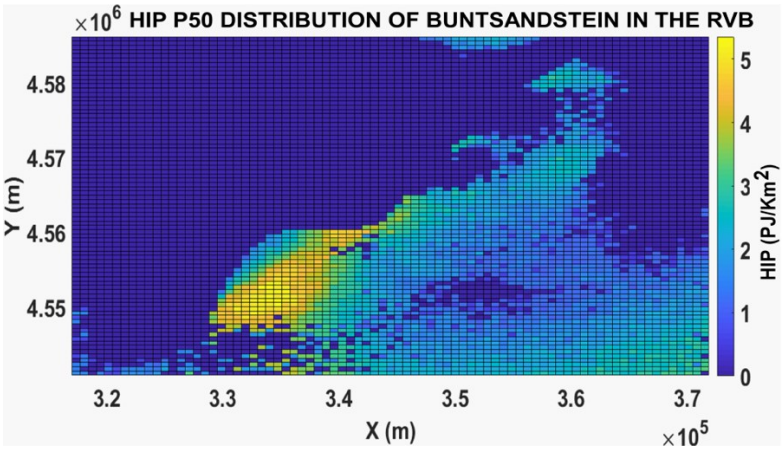

Figure 9: Example of P50 map with the HIP distribution for the Buntsandstein reservoir for the whole domain.

3.5 Discussion About the Workflow and the Results

As mentioned above, this study was not designed to give an accurate result of geothermal potential but to test the main workflow, which combines 3D models with the HIP method using a new MATLAB-based tool. The preliminary results show a first approximation of the HIP values and more importantly, where the high potential HIP regions for the Buntsandstein could be in the RVB basin. Thus, leaving aside the accuracy of the obtained results, it has become clear that the MATLAB HIP tool is already useful at the early stages of the assessment of the deep geothermal potential in an easy way. In this sense, results of HIP obtained from this tested case can be considered reasonable and will allow to address next works.

4. CONCLUSIONS

In this work, we evaluated the workflow for the assessment of the deep geothermal potential for the case study of Reus-Valls Basin (RVB) in the NE of Spain. This evaluation was done firstly by means of building a preliminary 3DGM using the current geological information, followed by refinement through a gravity/magnetic inversion to then construct a 3DTM through a quasi-stochastic approximation. Finally, these data were used to test a new MATLAB-based tool to calculate the "Heat in Place" using Monte Carlo simulations. This tool is able to evaluate de HIP potential for the entire unit (or a region of it) as well as it plots the results in a map format, which is able to be exported to GIS tools, to see the high potential regions even in the first phases of the assessment of the deep geothermal potential. Although this work presents a preliminary result, the geological model is still improving with the incorporation of new field data, so the results must be considered as preliminary. The workflow will be reused at a more advanced stage of 3D modelling for the evaluation of deep geothermal potential in this area.

Despite being a test case, the obtained results indicate this is a useful tool to evaluate the deep geothermal potential in early stages when the uncertainty in the potential geothermal reservoir does not allow more accurate results. Thus, the next step is applying this workflow in other cases for the assessment of deep geothermal resources in Catalonia, for conduction-dominated geothermal plays. This will allow to improve the workflow but, more importantly, to obtain a tool for systematising of the deep geothermal resource assessment.

REFERENCES

Aurensa. Estudio de Viabilidad de Estructura Proyecto de Almacenamiento Subterraneo de Gas Natural en Reus. (1996) Enagas, technical report.

Ayala, C., Torne, M., and Roca, E. A review of the current knowledge of the crustal and lithospheric structure of the Valencia Trough Basin. Boletín Geológico y Minero, 126 (2-3) (2015a): 533-552.

Ayala et al. Basement characterisation and cover deformation of the Linking Zone (NE Spain) from 2.5D and 3D geological and geophysical modelling. Proceedings, 8th EUREGEO (2015b), ICGC, Barcelona, Spain, pp 5-6.

Breede K, Dzebisashvili K, Liu X, Falcone G. A systematic review of enhanced (or engineered) geothermal systems: past, present and future. Geothermal Energy. (2013) 1:1–27. https://doi.org/10.1186/2195-9706-1-4

Cabrera, L., & Calvet, F. Onshore Neogene record in NE Spain: Vallès-Penedès and el Camp half-grabens (NW Mediterranean). Tertiary basins of Spain, 97-105 (1996). https://doi.org/10.1017/CBO9780511524851.017

Čermák, V. and Rybach, L. (1982). Thermal Conductivity and Specific Heat of Minerals and Rocks. In: M. Beblo, A. Berktold, U. Bleil, H. Gebrande, B. Grauert, U. Haack, V. Haak, H. Kern, H. Miller, N. Petersen, J. Pohl, F. Rummel and J. R. Schopper (Eds.): Landolt-Bornstein Numerical Data and Functional Relationships in Science and Technology, New Series, Group V, Geophysics and Space Research. Geophysics - Physical Properties of Rocks, 305–343, Springer, Berlin.

Clark, D. A. Magnetic petrophysics and magnetic petrology: aids to geological interpretation of magnetic surveys. Journal of Australian Geology and Geophysics, (1997) 17:83-103.

Colmenar-Santos, A. et al. The geothermal potential in Spain. Renewable and Sustainable Energy Reviews 56 (2016) 865–886. https://doi.org/10.1016/j.rser.2015.11.070

Fernàndez, M. Determinació de gradients geotèrmics a Catalunya. Gènsesi de les anomalies i interpretación del règim tèrmic. Ph.D thesis. University of Barcelona, Barcelona, Spain, (1988) 182 pp.

Garg, S. K., and Combs, J. Appropriate use of USGS volumetric "Heat in place" method and Monte Carlos calculations. Thirty-Fourth Workshop on Geothermal Reservoir Engineering Standford University, Stanford, California, February 1-3. (2010) SGP-TR-188.

Garg, S. K., and Combs, J. . A re-examination of USGS volumetric "Heat in Place" method. Proceedings, Thirty-Sixth Workshop on Geothermal Reservoir Engineering Standford University, Stanford, California, January 31 – February 2. (2011) SGP-TR-191.

Garg, S.G., and Combs, J.: A reformulation of USGS volumetric "heat in place" resource estimation method, *Geothermics*, **55**, (2015), 150–158. http://dx.doi.org/10.1016/j.geothermics.2015.02.004

Gomez-Gras, D. M. El Permotrías de las Baleares, de la cordillera Costero-Catalana y de la vertiente mediterránea de la cordillera Ibérica: Facies y petrología sedimentaria. Ph.D thesis, Autonomous University of Barcelona, (1992) 247pp.

Hasterok, D., Gard, M., and Webb, J. Geoscience Frontiers on the radiogenic heat production of metamorphic, igneous, and sedimentary rocks. Geoscience Frontiers, 9(6), (2018) 1777-1794. https://doi.org/10.1016/j.gsf.2017.10.012

ICGC. Geothermal Atlas of Catalonia: Geoindex-Deep-geothermal. (2012) http://www.icgc.cat/

ICGC. Model geològic 3D 1:250.000 M2010-13. (2013) http://www.icgc.cat/

ICGC. Mapa estructural de Catalunya 1:250 000. ICGC, Barcelona, España. (2014) http://www.icgc.cat/

IGME. Mapa Geológico de España E. 1:50.000. Hoja de Valls. Serie Magna. (1973) IGME, Madrid, España.

IGME. Mapa Geológico de España E. 1:50.000. Hoja de Reus. Serie Magna. (1980) IGME, Madrid, España.

Lukosevicius, V. Thermal energy production from low temperature geothermal brine – technological aspects and energy efficiency. (1993). ONU Geothermal Training Programme, Orkustofnum –National Energy Authority, Grensasvegur 9, 108 Reykjavik, Iceland.

Marzo, M. El Buntsandstein de los Catalánides: Estratigrafía y procesos sedimentarios. PhD thesis. University of Barcelona, Barcelona, Spain, (1980) 317pp.

Masana, E. L'activitat neotectònica a les Cadenes Costaneres Catalanes. PhD thesis. University of Barcelona, Barcelona, Spain, (1995) 450 pp.

Moeck, I.S.: Catalog of geothermal play types based on geologic controls, *Renewable and Sustainable Energy Reviews*, **37**, 867-882, (2014). http://dx.doi.org/10.1016/j.rser.2014.05.032

Muffler, L.J.P., and Cataldi, R.: Methods for Regional Assessment of Geothermal Resources, Geothermics, 7, (1978), 53-89. https://doi.org/10.1016/0375-6505(78)90002-0

Oldenburg, C., and Rinaldi, A.P. (2010). Buoyancy Effects on Upward Brine Displacement Caused by CO_2 Injection. Transport in Porous Media, 87(2), 525-540. https://doi.org/10.1007/s11242-010-9699-0

Tester JW, Anderson BJ, Batchelor AS, et al. The future of geothermal energy - impact of enhanced geothermal systems (EGS) on the United States in the 21st Century. MIT - Massachusetts Institute of Technology. (2006) p. 358.

Willems, C.J. L., and Nick, H. M. Towards optimisation of geothermal heat recovery: An example from the West Netherlands Basin. Applied Energy 247 (2019) 582-593. https://doi.org/10.1016/j.apenergy.2019.04.083

Wellman, J. F., and Regenauer-Lieb, K. Uncertainties have a meaning: Information entropy as a quality measure for 3-D geological models. Tectonophysics, (2012) 526-529, 207-216. https://doi.org/10.1016/j.tecto.2011.05.001